Authors' Instructions
Preparation of Camera-Ready Contributions to SCITEPRESS Proceedings

First Author Name[1], Second Author Name[1] and Third Author Name[2]
[1]*Institute of Problem Solving, XYZ University, My Street, MyTown, MyCountry*
[2]*Department of Computing, Main University, MySecondTown, MyCountry*
{f_author, s_author}@ips.xyz.edu, t_author@dc.mu.edu

Keywords: The paper must have at least one keyword. The text must be set to 9-point font size and without the use of bold or italic font style. For more than one keyword, please use a comma as a separator. Keywords must be titlecased.

Abstract: Operational maturity of biological control systems have fuelled the inspiration for a large number of mathematical and logical models for control, automation and optimisation. The human brain represents the most sophisticated control architecture known to us and is a central motivation for several research attempts across various domains. In the present work, we introduce an algorithm for mathematical optimisation that derives its intuition from the hierarchical and distributed operations of the human motor system. The system comprises global leaders, local leaders and an effector population that adapt dynamically to attain global optimisation via a feedback mechanism coupled with the structural hierarchy. The hierarchical system operation is distributed into local control for movement and global controllers that facilitate gross motion and decision making. We present our algorithm as a variant of the classical Differential Evolution algorithm, introducing a hierarchical crossover operation. The discussed approach is tested exhaustively on standard test functions as well as the CEC 2017 benchmark. Our algorithm significantly outperforms various standard algorithms as well as their popular variants as discussed in the results.

1 INTRODUCTION

2 Introduction

Evolutionary algorithms are classified as meta-heuristic search algorithms, where possible solution elements span the n-dimensional search space to find the global optimum solution. Over the years, natural phenomena and biological processes have laid the foundation for several algorithms for control and optimization that have highlighted their applicability in solving intricate optimization problems. For instance, at the cellular level in the E.Coli Bacterium, there is sensing and locomotion involved in seeking nourishment and avoiding harmful chemicals. These behavioral characteristics fuelled the inspiration for the Bacterial Foraging Optimization algorithm (**?**)(**?**). Ant Colony Optimization (**?**) deals with behavior of ants and has been a successful model for solving complex problems. Particle Swarm Optimization (**?**) is a swarm intelligence algorithm based on behavior of birds and fishes that models these particles as they traverse an n-dimensional search space and share information in order to obtain global optimum. From a biological control point, the human brain represents one of the most advanced architectures and several research attempts seek to mimic its functional accuracy, precision and efficiency. The brain function activities can be broadly classified into 2 categories: sensory and motor operations. Sensory cortical functions inspired the concept of neural networks that are being scaled successfully in deep learning to solve vast amount of problems.

The human motor function represents a distributed neural and hierarchical control system. It can be classified as having local control functions for movement as well as higher level controllers for gross motion and decision making. The execution of motor operation involves distributed brain structures at different levels of hierarchy. These include the pre-frontal cortex, motor cortex, spinal cord, anterior horn cells etc (**?**). For executing an action sequence, a sequence of actions is implemented by a string of subsequences of actions each implemented in a different part of the body. The operational structure has been depicted in Figure 1(**?**). For optimality of actions, neurons act

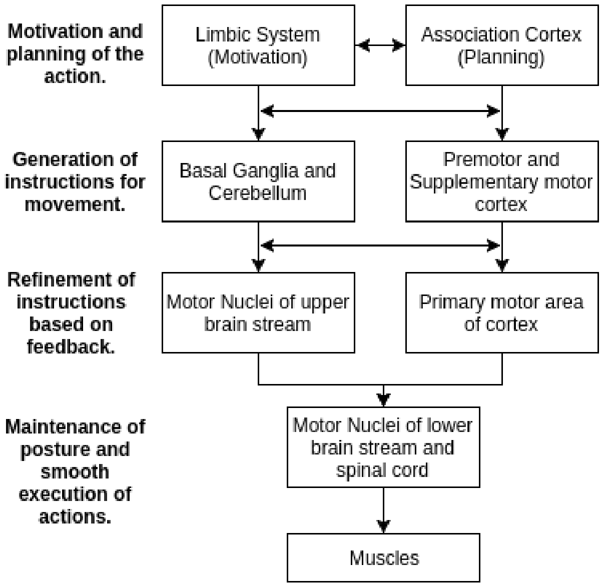

Figure 1: Hierarchy of Motor Control in Humans

in unison. The neurons in the motor cortex act like global leaders and send inhibitory or facilitatory influence over anterior horn cells, the local leaders, located in the spinal cord(**?**). These local leaders are connected to muscle fibers, the effectors, through a peripheral nerve and neuromuscular junction. Efficient execution of task requires feedback based facilitation and inhibition of the effectors over the anterior horn cells. These sequence of operations realise the optimal convergence of the system leading to smooth motor execution.

The present work introduces an algorithm modelled intuitively on the distributed and hierarchical operation of the brain motor function.

The Classical DE Algorithm (**?**), proposed by Storn and Price has been hailed as one of the premier evolutionary algorithms, owing to its simple yet effective structure(**?**). However, in recent times, it has been criticized for its slow convergence rate and inability to effectively optimize multimodal composite functions(**?**). This work focusses on supplementing the algorithm's performance through the introduction of hierarchical influence in the pipeline. The architecture enables the algorithm to control the flow of agents through the cummulative effect of global and local leaders in the hierarchy.
The proposed approach, Hierarchy Influenced Differential Evolution (HIDE), has been subjected to exhaustive analysis on the hybrid and composite objective functions of the CEC 2017 benchmark(**?**). Comparison with the classical DE algorithm and its other popular variants including JADE and PSODE (**?**) highlights the particular viability of the schemed approach in solving complex optimization tasks. We show that even with fixed parameters, HIDE is able to outperform adaptive architectures such as JADE by a respectable margin, as discussed in the result sections.

3 Classical Differential Evolution

The classical Differential Evolution (DE) algorithm is a population-based global optimization algorithm, utilizing a crossover and mutation approach to generate new individuals in the population for achieving optimum solutions(**?**). For each individual x_i that belongs to the population for generation G, DE randomly samples three individuals from the population namely $x_{r1,G}$, $x_{r2,G}$ and $x_{r3,G}$. Employing these randomly chosen points, a new individual trial vector, v_i, is generated using equation (1):

$$v_i = x_{r1,G} + F(x_{r2,G} - x_{r3,G}) \quad (1)$$

Where, F is called the differential weight (Usually lies between $[0,1]$).
To obtain the updated position of the individual, a crossover operation is implemented between $x_{i,G}$ and v_i, controlled by the parameter CR called the crossover probability. The value for CR always lies between $[0,1]$.

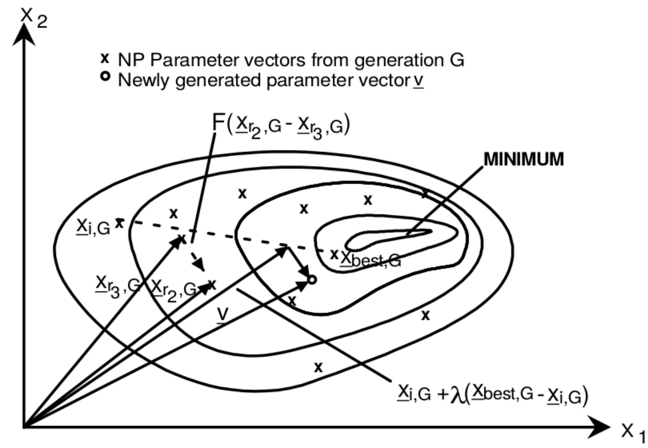

Figure 2: Motion planning of individuals in DE on two dimensional example of objective function.

4 Hierarchy Influenced Differential Evolution

Taking inspiration from the human motor system, we model the hierarchical motor operations in our optimization agents, where we define a global leader which influences the action of several distributed local leaders and the particle agents which act as the effectors. The global leader is analogous to the decision making and planning section in the motor system hierarchy whilst, the local leaders correspond to motion generators acting under the influence of the global leader.

The position of each particle in the population is affected by the influence of global leader and local leaders, while also being affected by a randomly chosen particle from the population to induce some stochasticity in the optimization pipeline. We first model the influence of the global leader on the local leaders and the influences of the local leaders on each population element using equation (2) and (3). We introduce a hierarchical crossover between the two influencing equations governed by a hierarchical crossover parameter HC.

Analogously to the brain motor operation as depicted in Figure 1, the update of particle positions requires generating feedback for the leaders as a part of the optimization procedure, and hence the local leaders and the global leader are updated based on their objective function value generated from the perturbations in population particles. This series of events comprise of one optimization pass (one generation step). On execution of several optimization passes as described, the system is able to converge to an optimal configuration, analogous to the successful execution of the required task as shown in the final steps of Figure 1.

For each particle $x_{i,G}$, $i = 0, 1, 2, ...NP-1$ for generation G, the trial vector x_i' of the particle, is governed by the hierarchical crossover operation and a mutation operation as follows :

$$u_i = \begin{cases} E_g, & if\ G < HC * G_t \\ E_l, & otherwise \end{cases} \tag{2}$$

$$E_g = g_L + F(x_{L_i,G} - x_{r,G}) \tag{3}$$

$$E_l = x_{L_i,G} + F(x_{i,G} - x_{r,G}) \tag{4}$$

for each dimension j of $x_{j,i,G}$:

$$x'_{j,i} = \begin{cases} x_{j,i,G} & if\ rand(0,1) < HC \\ u_{j,i} & otherwise \end{cases} \tag{5}$$

$$x_{i,G+1} = \begin{cases} x'_{i,G}, & if\ f(x'_{i,G}) < f(x_{i,G}) \\ x_{i,G}, & otherwise \end{cases} \tag{6}$$

where,
G_t is the total number of generations,
$x_{i,G+1}$ is the vector position of $x_{i,G}$ for next generation
F is factor responsible for amplification of differential variation,
f is the objective function,
$x_{i,G}$ is the current position of the individual for generation G,
u_i is the intermediate trial vector of the current individual,
E_g represents the global and local leader interaction,
E_l represents the local leader and effector interaction,
g_L is the global leader for generation G,
$x_{L_i,G}$ is the position of the local leader for current individual,
$x_{r,G}$ε P ; r ε [0,1,.. NP-1]
$x'_{j,i}$ is the trial vector

Algorithm 1 Hierarchy Influenced Differential Evolution

procedure START
  Initialize parameters (HC, F, P, N_l, NP).
  Generate initial global leader g_L as a random point.
  Generate N_l local leader points around g_L global leader.
  Using a Normal distribution, generate NP points for population P around the local leaders.
  while termination criteria is not met **do**
    for each individual $x_{i,G}$ in P **do**
      Determine the corresponding local leader $x_{L_i,G}$ from the set of all local leader based on nearest position.
      Let $u = 0$ be an empty vector.
      Let G and G_t be the current generation and total generations of the procedure.
      if $G == (HC * G_t)$ **then**
        Increase the population : $G_t = 2 * G_t$
      end if
      if $G < (HC * G_t)$ **then**
        $u_i = E_g$ from (2).
      else
        $u_i = E_l$ from (3).
      end if
      x_i' = BinomialCrossover(u_i, $x_{i,G}$, CR)
      if $f(x_i')$ ¡ $f(x_{i,G})$ **then**
        Replace $x_{i,G}$ with x_i' in the next generation.
      end if
    end for
    Alter local leaders in each population cluster based on objective function value.
    Compute updated global leader g_L.
  end while
end procedure

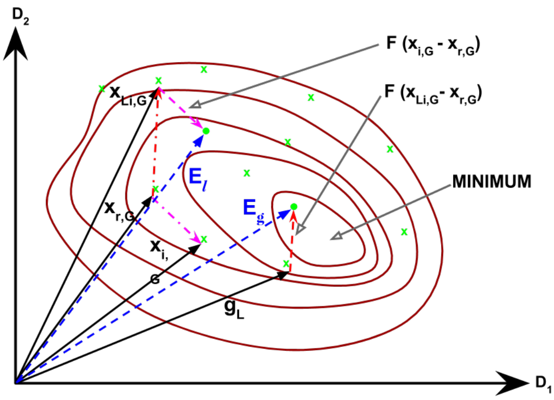

Figure 3: Hierarchical Decisive Motion planning of individuals in HIDE on two dimensional example of objective function. The position vectors resulting from the influence of global leader and local leaders are both represented as E_g and E_l on the contour of a two dimensional objective function.

$x_{r,G}$ is randomly chosen particle from the population to induce stochasticity. The hierarchical operation is affected by the global leader g_L and the local leader $x_{L_i,G}$ through the parametric equations (2) and (3). Switching between the two is governed by the hierarchical crossover parameter HC.

4.1 Hierarchical Crossover

Convergence trend in HIDE is largely pivoted about (3) and (4), which in unison, lend a hierarchical structure to the algorithm. A successful optimization algorithm involves establishing a trade-off between exploration and exploitation. Achieving global optimization can be visualized as collaboration of two forces,

Algorithm 2 Binomial_Crossover(u, x, CR)

procedure START
  Let $x' = 0$ be an empty vector.
  Select a random integer k = $irand(\{1,2,...,d\})$; where d = number of dimensions
  for each dimension j **do**
    if $random(0,1) < CR$ **or** $j == k$ **then**
      Set $x'_j = u_j$
    else
      Set $x'_j = x_j$
    end if
  end for
end procedure

exploration over a larger subspace followed by intensive exploitation over the resulting search space governed by clusters. Phase 1, involving (3) is marked by the interaction between the global and local leaders representing decision planning and facilitation of gross motion. This is followed by phase 2, involving (4) wherein the local leaders interact with and guide their effector population to control intricate motion over the constraint subspace to achieve smooth convergence. Robust covergence necessitates an optimal transition from phase 1 to phase 2 in the hierarchy. This hierarchical transition is characterized by our proposed parameter, HC. **The value of HC belongs to [0,1]. An optimal value for HC was observed experimentally to lie about one-quarter. For the purpose of our experiment, we have deterministic fixed *HC* to be 0.27. The choice for *HC* was made after successful experimental observation on more than 50% of the test functions with *HC* set as 27% of the total generation budget.**

The HIDE algorithm achieves a performance improvement in the early optimization phase ($G < HC * G_t$) by replacing clusters of the initially generated candidate solutions with the locally best. This strategy rules out a number of mutation vectors that are more unfavorable in terms of performance gain. Additionally, by focusing on mutants of the globally best candidate solution the search space is explored rather quickly during this phase. After the population advances to $HC * G_t$ generations, the algorithm changes its reference point (the trial vector) to the locally best candidate solutions of a certain cluster. That is, having approached a closer distance from the optimal, the algorithm is able to exploit the search space. Our proposition is complemented by the observations in our results section wherein we significantly outperform several popular algorithms on involved multimodal hybrid and composite functions in higher dimensions.

5 Results and Discussions

All evaluations were performed using Python 2.7.12 with Scipy(**?**) and Numpy(**?**) for numerical computations and Matplotlib (**?**) package for graphical representation of the result data. This section is divided into two sub-sections: Section A provides description about the problem set used for analysis of algorithmic efficiency and accuracy, and section B comprises of tabular and graphical data to reinforce the claim of superiority of the proposed approach.

Table 1: CEC 2017 Test Functions

F_{id}	Problem Function	F*
f_1	Shifted and Rotated Bent Cigar Function	100
f_2	Shifted and Rotated Sum of Different Power Function	200
f_3	Shifted and Rotated Zakharov Function	300
f_4	Shifted and Rotated Rosenbrock's Function	400
f_5	Shifted and Rotated Rastrigin's Function	500
f_6	Shifted and Rotated Expanded Scaffer's F6 Function	600
f_7	Shifted and Rotated Lunacek Bi_Rastrigin Function	700
f_8	Shifted and Rotated Non-Continuous Rastrigin's Function	800
f_9	Shifted and Rotated Levy Function	900
f_{10}	Shifted and Rotated Schwefel's Function	1000
f_{11}	Hybrid Function 1 (N=3)	1100
f_{12}	Hybrid Function 2 (N=3)	1200
f_{13}	Hybrid Function 3 (N=3)	1300
f_{14}	Hybrid Function 4 (N=4)	1400
f_{15}	Hybrid Function 5 (N=4)	1500
f_{16}	Hybrid Function 6 (N=4)	1600
f_{17}	Hybrid Function 7 (N=5)	1700
f_{18}	Hybrid Function 8 (N=5)	1800
f_{19}	Hybrid Function 9 (N=5)	1900
f_{20}	Hybrid Function 10 (N=6)	2000
f_{21}	Composition Function 1 (N=3)	2100
f_{22}	Composition Function 2 (N=3)	2200
f_{23}	Composition Function 3 (N=4)	2300
f_{24}	Composition Function 4 (N=4)	2400
f_{25}	Composition Function 5 (N=5)	2500
f_{26}	Composition Function 6 (N=5)	2600
f_{27}	Composition Function 7 (N=6)	2700
f_{28}	Composition Function 8 (N=6)	2800
f_{29}	Composition Function 9 (N=3)	2900
f_{30}	Composition Function 10 (N=3)	3000
Search Range: $[-100,100]^D$		

5.1 Problem Set Description

The set of objective functions considered for testing the proposed algorithm and compare its performance against classical DE and its variants PSODE and JADE have been taken from the CEC 2017 set of benchmark functions. Exhaustive comparisons and analysis have been depicted on dimensions D = 10, 30, 50 and 100 for a clear understanding of the strengths of the proposed algorithm. Objective functions $f_1 - f_3$ are simple unimodal functions and $f_4 - f_{10}$ are multimodal functions with a high number of local optima values. Functions $f_{11} - f_{20}$ are all hybrid functions using a combination of functions from $f_1 - f_{10}$. The set of composite function range from $f_{21} - f_{30}$ and merges the properties of the sub-functions better while incorporating the basic functions as well as hybrid functions to increase complexity while maintaining continuity around the global optima.

Summarized in Table 1 are the 30 objective functions from the CEC 2017 dataset and the global optimum value for each function denoted by $F*$. In all simulation runs, we set the population size NP to a fixed value of 100, and the results are shown in a tabular structure depicting the best and average values of the population individuals for the simulations. Additionally, several graphical results have been discussed to observe the convergence rate and efficiency of the algorithms used in the simulation. These graphs were plotted based on the numerical results obtained from the simulation runs used to build the tables.

5.2 Parameter Settings

For fair comparisons, the parameters for all algorithms are fixed to the values depicted in table 2. As clear from the table, we set the parameters F and CR as 0.5 and 0.9 for DE across all experiments, as recommended in (**?**),(**?**),(**?**). The parameters for JADE were selected as suggested in the original work(**?**). These parameter settings allow transparency in results and a base for fair and clear comparisons in the analysis of the algorithms.

Table 2: Algorithm Parameter Settings used for comparision

Algorithm	Parameter	Value
2*DE (**?**),(**?**),(**?**)	F	0.5
	CR	0.9
5*PSODE ()	w	0.7
	Cp	2.0
	Cg	2.0
	F	0.48
	CR	0.5
2*JADE (**?**)	μ_{CR}	0.5
	μ_F	0.5
3*HIDE	HC	0.27
	F	0.48
	CR	0.9
	N_l	5

Table 3: Objective Function Value for Dimension: 10

ID	DE		JADE		PSO-DE		HIDE	
	best	mean	best	mean	best	mean	best	mean
f_1	100.000051	100.011085	**100.0**	**100.0**	100.000712	185.975885	**100.0**	**100.0**
f_2	**200.0**	200.1	**200.0**	**200.0**	**200.0**	**200.0**	**200.0**	**200.0**
f_3	300.00134	300.214502	**300.0**	**300.0**	300.000006	300.000985	**300.0**	**300.0**
f_4	400.042617	403.674837	**400.0**	400.409399	400.064644	404.307763	**400.0**	**400.000003**
f_5	566.661791	604.867489	**523.908977**	**541.521084**	525.868824	575.61616	533.803201	579.483815
f_6	621.914237	634.807962	620.878276	636.034759	**603.187964**	635.865001	613.730565	**629.293758**
f_7	724.831278	739.129935	**717.016542**	**723.983312**	725.44788	733.15638	720.345706	725.233785
f_8	**818.904202**	829.749207	821.914433	**826.321588**	820.8941	830.246691	821.064763	828.160987
f_9	**900.0**	908.104383	**900.0**	1084.478253	**900.0**	1124.102561	**900.0**	**903.454324**
f_{10}	1911.510092	2447.443751	1760.956867	2162.648588	2049.644727	2518.241095	**1694.437597**	**2049.074266**
f_{11}	1102.985708	1113.423105	1105.661676	1117.509748	1105.97013	1120.192974	**1101.769749**	**1108.863598**
f_{12}	2531.746305	6509.743078	1438.605713	5430.674683	4089.006352	10810.387667	**1308.438341**	**1327.405881**
f_{13}	1313.130226	1404.903601	**1304.681558**	**1328.755262**	1319.839199	1453.340785	1306.682039	1344.282241
f_{14}	1409.949612	1426.571937	1412.934432	1428.169439	1420.91065	1434.112884	**1404.928993**	**1410.000769**
f_{15}	1504.131392	1521.446614	1502.496189	1508.31154	1501.389515	1518.310358	**1500.08137**	**1503.169264**
f_{16}	1958.42062	2104.555728	1958.857997	2094.630816	**1958.411527**	**2048.156879**	1958.433511	2062.385949
f_{17}	1728.194973	**1743.155244**	1730.715318	1748.129878	1727.80039	1791.607742	**1723.853972**	1747.589077
f_{18}	1801.586012	1838.840555	1804.298538	1825.091639	1817.154641	1840.546923	**1800.235516**	**1804.014301**
f_{19}	1901.195482	1903.604767	1900.399786	1902.152965	1902.71174	1906.252333	**1900.005632**	**1901.014116**
f_{20}	2204.55412	2289.226577	2148.538938	2178.313173	2140.561308	2261.038768	**2139.915527**	**2172.816519**
f_{21}	2337.772994	2387.230357	**2314.421135**	**2338.688719**	2337.207339	2351.898856	2320.496212	2344.61612
f_{22}	2300.805852	2304.132879	**2300.0**	**2300.093485**	2300.684181	2301.710478	2300.000015	2301.095975
f_{23}	3070.177083	3145.772296	3003.678563	3091.22041	**2773.372859**	3060.022519	2867.020036	**3047.982305**
f_{24}	**2500.0**	**2500.0**	**2500.0**	**2500.0**	**2500.0**	**2500.0**	**2500.0**	**2500.0**
f_{25}	2899.584968	2933.249812	2899.584968	2930.266506	**2897.742869**	**2921.27479**	2897.833388	2927.976511
f_{26}	**2800.0**	4117.597033	**2800.0**	**2956.064173**	**2800.0**	3367.60765	**2800.0**	3161.548079
f_{27}	3113.157656	3358.806434	3072.439023	3178.509645	3078.873134	3240.501812	**3071.203569**	**3107.268539**
f_{28}	3184.75565	3230.921422	3184.75565	**3195.113042**	3184.755652	3198.370691	**3100.0**	3195.411961
f_{29}	**3148.587115**	3266.979786	3172.400194	**3233.707677**	3191.348193	3244.892638	3189.211417	3292.420474
f_{30}	3442.555095	11927.404685	3207.766942	4615.591316	4573.358512	16415.162901	**3205.740954**	**3249.710975**
$w/t/l$	2/4/24	1/1/28	5/7/18	9/4/17	4/4/22	2/2/26	12/7/11	14/4/12

5.3 Numerical and Graphical Results

In tables 3-6, the best and mean values obtained for the population agents in the simulation runs have been reported, and the optimum values for each objective function have been highlighted in **bold**. For the sake of clarity, the comparison results in each table have been summarized in "$w/t/l$" format wherein w represents the number of objective functions where the algorithm outperforms all other algorithms, t specifies the number of objective functions where it is tied as the best algorithm for the objective function and l represents the number of test functions where it does not finish first. The utilization of the evaluation metric facilitates a definitive comparison of the different algorithms under consideration.

Tables 3 and 4 highlight the performance of the algorithms for $D = 10$ and $D = 30$ respectively. For $D = 10$, HIDE depicits impressive performance. It registered a "$w/t/l$" score of $12/7/11$ in the best case and $14/4/12$ in the mean of population case. In both these test functions, JADE achieved the second best performance registering a w/t/l of $5/7/18$ on the best optimal value case and $9/4/17$ on the mean of optimal value case. On $D = 30$, HIDE achieved maximum number of wins in both best and mean case (17 and 18 respectively). JADE achieved second position with 8 and 9 wins in the best and mean case. The decent performance of JADE can be attributed to the adaptive nature of its parameter selection which enables enhancement of its convergence rate.

The results for $D = 50$ and $D = 100$ (higher dimensions) have been summarized in tables 5 and 6. On $D = 50$, HIDE depicted exceptional performance, outperforming all other algorithms. It registered 17 wins in the best case and 18 wins in the mean case. Classical DE shows no wins in any case in high dimensional settings owing to its slow convergence rate and inability to attain global optimum thus highlighting the usefulness of the modifications introduced in the variants including HIDE. Similarly for $D = 100$, HIDE again outperforms all other algorithms by an appreciable margin. From a functional standpoint, It would be worthwhile to highlight that HIDE outperformed the other 3 compared algorithms on majority on the composite and hybrid functions, particularly on the higher dimensional settings. The efficiency of HIDE can be attributed to the hierarchical nature of crossover selection and concurrency in vector configurations at the higher hierarchy levels. The

Table 4: Objective Function Value for Dimension: 30

f_{id}	DE		JADE		PSO-DE		HIDE	
	best	mean	best	mean	best	mean	best	mean
f_1	100.001508	4334.438478	100.001338	100.056201	364.295574	4236.363207	**100.0**	**100.0**
f_2	40412441.0	5.129601e+19	**200.0**	1535352368.	6332899.0	9.590679e+11	**200.0**	**159855.5**
f_3	17926.87287	322131.54271	969304.92609	174080.70037	215792.54757	521683.209092	**3679.811599**	**8999.947269**
f_4	481.255055	519.422652	403.633939	**442.206911**	468.341175	479.341966	**400.004163**	443.016156
f_5	689.041352	737.79326	**667.50756**	**735.204027**	715.904429	746.548906	685.40454	738.842184
f_6	**643.626307**	652.582714	651.39169	655.142819	642.724237	655.106996	644.701241	**652.002395**
f_7	883.347367	962.591129	**779.907693**	**818.344111**	790.014281	854.285524	812.923573	856.90477
f_8	923.37426	967.251501	931.500175	**957.362003**	**915.414882**	960.486239	930.288539	964.11663
f_9	5652.483961	7878.781444	4953.05469	5146.600953	6018.417197	9042.410178	**4003.118072**	**4734.984364**
f_{10}	**3596.63104**	4536.989761	4012.723292	**4204.18969**	3934.606704	4863.741107	3793.781776	4346.741344
f_{11}	1162.405965	1184.634006	1152.748529	1174.58813	1165.144993	1189.171787	**1149.748499**	**1171.130409**
f_{12}	56679.43509	2317650.6134	924821.17176	558930.09024	210221.07746	5161046.05540	**9208.289246**	**41947.22269**
f_{13}	3002.029489	18794.83599	14276.907742	13775.81623	93871.279833	10612.26359	**1664.06241**	**2453.606969**
f_{14}	1773.180798	5502.160382	1496.219858	42868.9158	1555.452763	4029.808535	**1462.926848**	**1504.191515**
f_{15}	1860.435669	2484.689969	1688.05046	2222.674323	1651.747476	2223.060542	**1611.074402**	**1852.66177**
f_{16}	2517.439623	2827.004968	2344.19818	2621.618684	**2239.242719**	**2664.114667**	2298.041965	2691.674809
f_{17}	2321.175936	2604.529778	2062.898023	2546.995596	2107.43677	2457.34021	**1820.806639**	**2418.723829**
f_{18}	38987.28245	694156.328505	**11841.60813**	184888.1621	862294.85325	7118430.2891	212578.003784	**23024.11193**
f_{19}	2043.469888	3010.235379	1959.71819	2156.957875	3049.52231	6840.408394	**1949.271714**	**1987.866761**
f_{20}	2625.539158	2864.832611	**2706.314441**	**2805.600064**	2619.996493	2895.107238	2753.806213	2966.035793
f_{21}	2412.081757	2504.777775	2414.52134	2456.718982	2431.740293	2478.841357	**2200.0**	**2442.734316**
f_{22}	2300.481796	5655.569322	**2300.0**	**4157.698784**	2307.721358	6811.069162	2300.009985	6795.24842
f_{23}	3050.654508	3572.965066	**2772.002023**	**2946.749322**	2764.922461	3199.874364	2883.276891	3543.839343
f_{24}	3104.623692	3290.698756	2891.557648	2965.225566	**2911.63347**	2983.772932	**2500.0**	2940.75997
f_{25}	2916.180657	2946.711753	2875.106846	2881.091389	2875.498843	2889.943671	**2874.171109**	**2877.484904**
f_{26}	4043.691403	6756.3724	2900.0	**3266.510982**	**2800.007809**	3273.128769	2900.0	3298.490539
f_{27}	3200.005857	3998.876498	3145.810354	**3189.82261**	3145.425231	3639.634132	**3132.816283**	3284.28897
f_{28}	3290.744025	3326.263983	**3100.0**	3131.027315	3195.486838	3225.594053	**3100.0**	**3115.505829**
f_{29}	3720.314598	4115.185803	**3305.310139**	**3626.887552**	3535.952295	3867.593068	3352.845055	3709.102375
f_{30}	3359.030768	3900.826662	**3263.496536**	3749.610722	3312.635025	3524.714477	3298.704645	**3421.715322**
$w/t/l$	2/0/28	0/0/30	8/2/20	11/0/19	4/0/26	1/0/29	15/2/13	17/0/13

tabular results reinforce the fact that HIDE outperforms JADE, PSODE and DE. On close analysis, it can be witnessed that HIDE falls behind the other algorithms on a small fraction of unimodal functions such as f_5, f_7 on lower dimensions due to fast convergence during early stages of execution. However, the performance of higher dimensions, particularly on the more involved functions highlights utility for real world problems.

The tabular results are complemented through the graphical representations in Figure 4. For the sake of clarity, representations of higher dimensional problems span more number of iterations than those for lower dimensional settings. Analysis of the plots clearly depicts that HIDE shows better convergence rate as compared to other algorithms. As the analysis transcends to higher dimensional settings, the proposed approach outperforms the other algorithms on majority of the objective functions with respect to both convergence rate and optimality. the superiority of our algorithm in higher dimensions (50 and 100) is clearly evident from Figure 4. (m,n,q,r,s,t). Figure 4. (e,f,g,h) depict that for functions where HIDE and the other variants may depict similar trends on lower dimensions, HIDE eventually excels and surpasses them in higher dimensions in most scenarios. Almost all figures are representative of a faster convergence rate for HIDE on higher dimensions. This remarkable trait in HIDE enhances its utility for high dimensional problems where fast convergence to global optimum value is required, hence making it superior to the other considered algorithms and several variants of the DE algorithm.

6 Conclusion

Differential Evolution has been regarded as one of the most successful optimization algorithms and over the years, several variants have been proposed to enhance its convergence rate and performance. In the present work, we introduced a hierarchy influenced variant of the classical DE algorithm and modeled the same on the brain motor operation. The algorithm was characterized by global leader, local leaders and an effector population. The global leader and distributed local leaders interacted to facilitate gross motion via a greedy exploration strategy. The local leaders and their effectors interacted to control intricate motion for smooth convergence. A hierarchical

Table 5: Objective Function Value for Dimension: 50

f_{id}	DE		JADE		PSO-DE		HIDE	
	best	mean	best	mean	best	mean	best	mean
f_1	5884574.8731	4367294248.5	2136.072384	3708.75086	5811.218992	154233.64674	**406.072862**	**3665.419272**
f_2	4.718137e+24	3.364977e+44	**2635725.0**	**5.02374e+26**	2.212101e+19	2.544543e+23	2.279950e+17	1.00729e+31
f_3	45520.96637	662237.29681	9143481.79314	756166.76235	62308.42743	64435.24063	**44613.29993**	**58182.83733**
f_4	574.400328	801.384952	418.580378	470.113207	477.080964	574.528479	**400.005049**	**447.775413**
f_5	816.394775	843.258843	809.899483	834.131266	**778.59312**	831.066954	791.405194	**830.218472**
f_6	652.541914	655.794152	**633.217881**	**654.893828**	653.291336	658.183613	645.25633	656.060597
f_7	1109.02123	1263.038487	**889.036574**	**944.90319**	915.153525	1047.43879	989.957862	1186.248741
f_8	1139.278925	1175.893113	1118.339103	**1144.604745**	**1092.62639**	1159.032351	1100.476077	1168.529946
f_9	22196.38781	729218.77598	211958.280061	**13174.66236**	24753.04054	132233.95451	**10251.47631**	14752.7168
f_{10}	6228.49289	7289.183679	6054.707691	6833.306317	6207.795302	7055.595231	**6050.434374**	**6609.804567**
f_{11}	1170.858603	1258.517635	1202.694857	1232.204268	1206.154564	1252.939541	**1156.439606**	**1205.254497**
f_{12}	677263.0799	16987989.981	**74784.6159**	530814.6481	584300.6983	3448448.7906	126908.2157	**494471.0756**
f_{13}	6005.535308	16893.94992	12041.488125	4332.5945	1572.252973	**4301.829606**	**1484.761799**	7760.056137
f_{14}	38490.53231	5174367.45065	**2466.047056**	238838.47005	16327.42317	67939.00026	42967.818485	**26290.31618**
f_{15}	2278.141229	26989.25550	913553.04186	425636.76961	13443.587343	**9167.267098**	**1938.200405**	14976.72189
f_{16}	2722.026011	3176.916902	**2345.400708**	**2916.561016**	2521.93881	3146.04527	2436.449338	2978.37746
f_{17}	2799.949776	3289.61565	2568.383575	2907.869272	2887.281107	3236.957928	**2561.370306**	**2874.965038**
f_{18}	264037.1257	0872072.4773	936176.58677	**113941.3176**	**26965.28512**	114846.12136	260540.78181	936454.326476
f_{19}	10051.91240	720380.25713	2089.172253	7763.17234	9905.850822	16555.756926	**2013.126904**	**3609.258962**
f_{20}	2950.923195	3274.334015	3041.81309	3113.289461	2991.589293	3361.823946	**2495.031774**	**3080.137478**
f_{21}	2596.725663	2689.688363	2526.190898	2597.677199	2555.8788	2642.381597	**2447.758274**	**2570.911014**
f_{22}	9713.993241	10803.65373	210759.59674	11032.88095	38918.436264	10465.022457	**8181.446081**	**9755.070369**
f_{23}	3451.104943	4200.174424	2971.160647	3237.778662	2977.554961	3490.639751	**2851.650254**	**3162.313622**
f_{24}	3434.465028	3682.846708	3103.955173	3185.382676	**3036.799607**	**3158.330504**	3136.927747	3284.656095
f_{25}	3141.144886	3292.303449	2931.162959	2962.471758	2931.926959	3008.895353	**2931.142314**	**2954.767839**
f_{26}	4906.132848	7989.490966	**2900.0**	3346.874039	2900.441895	3653.757741	**2900.0**	**3262.668498**
f_{27}	3200.010703	3792.645588	3143.038057	3184.646353	3158.178238	3397.130323	**3141.010872**	**3176.011524**
f_{28}	3300.010827	3431.570911	**3240.725865**	**3288.253039**	3263.207144	3300.257609	3243.631996	3294.373237
f_{29}	3812.475517	4605.349537	**3533.945743**	**3956.835243**	3955.324537	4364.18129	3653.675553	3966.471956
f_{30}	3673.711968	5813.173755	3916.725719	4869.089335	3730.309354	5143.078706	**3346.483679**	**4747.88675**
$w/t/l$	0/0/30	0/0/30	8/1/21	9/0/21	4/0/26	3/0/27	17/1/12	18/0/12

crossover parameter was introduced to characterize the hierarchical transition between the two interactions. The influence of the vector configurations at the higher levels of hierarchy enabled the algorithm to avoid local minima in most objective functions. The same is complemented through our result observations wherein we significantly outperform several popular algorithm on complex multimodal functions in higher dimensional settings. Our proposed approach has sought to establish a viable tradeoff between fast optimization, robust convergence and low number of control parameters. The performance analysis of the algorithm highlights the particular effectiveness of the proposed approach on high dimensional hybrid and composite functions. The observed results provide sufficient motivation to extend the scope of the work to complex high dimensional real life problems including image enhancement, traveling salesman problem and flexible job-shop scheduling.

Table 6: Objective Function Value for Dimension: 100

f_{id}	DE		JADE		PSO-DE		HIDE	
	best	mean	best	mean	best	mean	best	mean
f_1	3427212811.79	13807281895.7	141.263356	13516.69893	36067123.52108	89751976.509	**122.398748**	**11708.82360**
f_2	4.19617e+84	1.54741e+112	8.73752e+74	2.54362e+87	**6.1536e+66**	**3.2118e+73**	3.8835e+80	8.8914e+114
f_3	228808.969094	262699.687639	912244.360944	332179.290693	241427.723667	257462.977882	**220765.0838**	**251901.1093**
f_4	1975.651157	2752.246068	539.386275	677.054657	777.314462	836.965399	**531.169819**	**621.219143**
f_5	1223.536503	1286.153332	1249.195036	1307.110127	1248.410134	1310.887657	**1068.11742**	**1272.47682**
f_6	651.650133	657.84974	654.709342	659.421427	656.877048	662.318417	**642.33355**	**654.132758**
f_7	1614.003864	1920.797726	1367.066537	1536.357878	**1311.849757**	**1534.207764**	1562.379772	2076.702502
f_8	1595.418732	1736.367379	1672.567849	1768.082435	1678.127263	1761.94051	**1293.552115**	**1592.162983**
f_9	59726.51462	171986.04390	528906.90908	30336.74533	563640.33135	174961.22099	**823466.57501**	**27067.02959**
f_{10}	12005.88972	114725.34833	414227.80190	915355.62189	112937.02785	714972.95073	**811153.58683**	**13298.09210**
f_{11}	7540.617987	11481.26014	540447.54868	857228.68366	**63521.901521**	**4544.804011**	5380.432052	9916.347692
f_{12}	529993877.325	1881773956.29	9893556.2722	**26415173.6097**	26105108.93	741876679.086	**23680108.181**	10059039.63
f_{13}	7943.9249	508209.56266	8622.698553	**8892.775994**	8246.515295	12675.84553	**52976.841354**	11376.986338
f_{14}	728122.833251	1329183.1722	**432194.7952**	**365560.8816**	548410.33828	9941547.52476	234045.94016	867160.306892
f_{15}	2660.465784	181957.06013	**31799.506503**	3362.509604	1899.073444	**2914.44348**	1976.789124	4485.415275
f_{16}	4749.254663	5847.826738	4817.483738	5632.3022	3852.700054	5228.663526	**3519.494945**	**4796.802728**
f_{17}	4397.496352	4958.418182	3842.206015	**4450.177422**	3790.72056	4730.994585	**3582.785882**	5463.216947
f_{18}	1357845.39305	1938893.27971	**146426.2736**	**763318.8226**	1004224.20382	2315010.29866	831040.14635	1335739.59138
f_{19}	2482.170159	26455.706954	2098.9496	4767.529535	2263.725158	3927.459947	**2071.077067**	**3664.159878**
f_{20}	4968.497438	5436.604051	5231.026486	5690.748998	5109.460563	5781.300835	**3627.777893**	**5228.430669**
f_{21}	3180.746656	3355.4783	2921.900122	**3085.692252**	**2885.574085**	3127.356835	2926.350399	3199.986183
f_{22}	17808.89774	419562.98664	619213.37566	820278.92909	318695.52231	220167.41374	**117548.33905**	**19547.15124**
f_{23}	4907.519646	5819.207866	**3352.556985**	4222.436894	3582.043556	4779.921248	3418.983204	**3609.098575**
f_{24}	5173.249408	5946.12042	4060.951302	4095.429519	**3801.368588**	**4042.426859**	3998.054028	4216.824895
f_{25}	4089.118918	4548.285768	**3153.485413**	**3236.61784**	3348.382262	3407.526581	3176.3038	3264.318532
f_{26}	8557.498566	20159.11458	2900.077371	11924.79947	33021.136025	8682.035439	**2900.000382**	**7867.5518**
f_{27}	3200.023355	3772.409153	**3194.809213**	3201.670732	3200.024171	3494.618132	3200.023542	**3200.023953**
f_{28}	4947.745152	5948.213156	**3295.122914**	**3340.280383**	3456.828432	3542.571307	3300.807691	3354.717338
f_{29}	6004.774424	7090.642544	5208.711727	5970.628689	5462.328635	6178.559061	**4541.195471**	**5739.291549**
f_{30}	7798.106217	202435555.59	**3584.974771**	10674.21733	13920.327039	**7139.460728**	3850.317099	15318.554601
$w/t/l$	0/0/30	0/0/30	8/0/22	8/0/22	5/0/25	6/0/24	17/0/13	16/0/14

0.24

(a) b

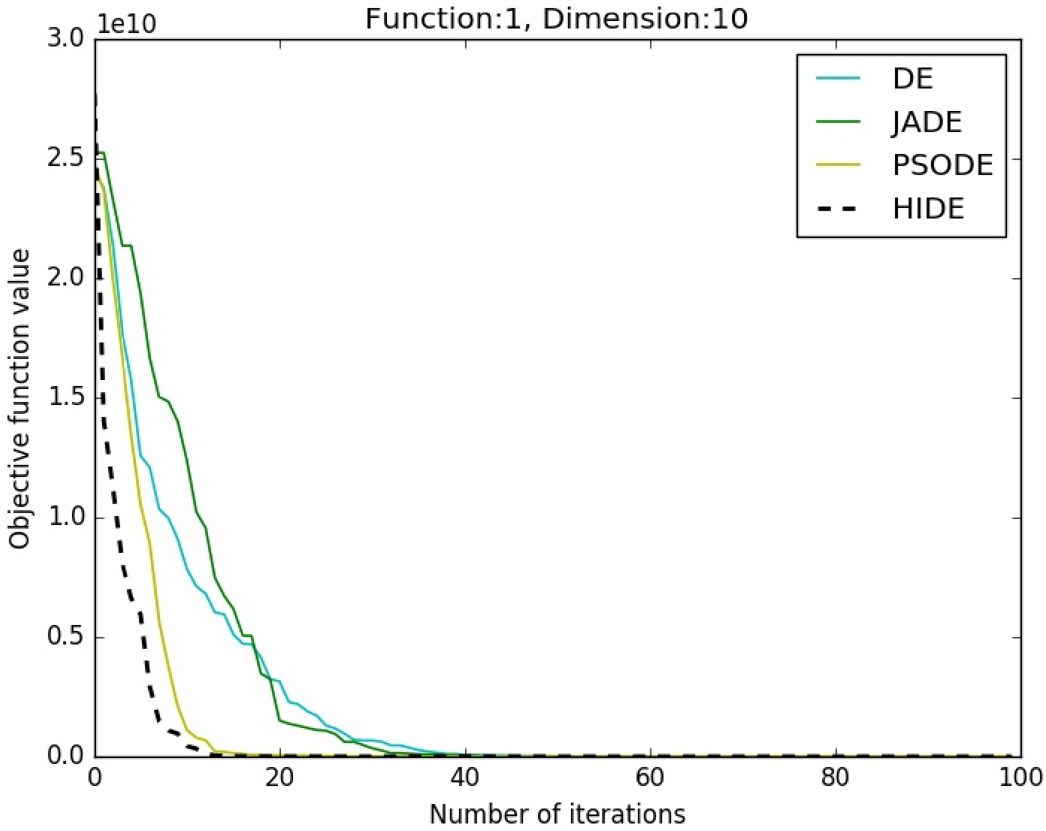

Figure 4

0.24

(a) b

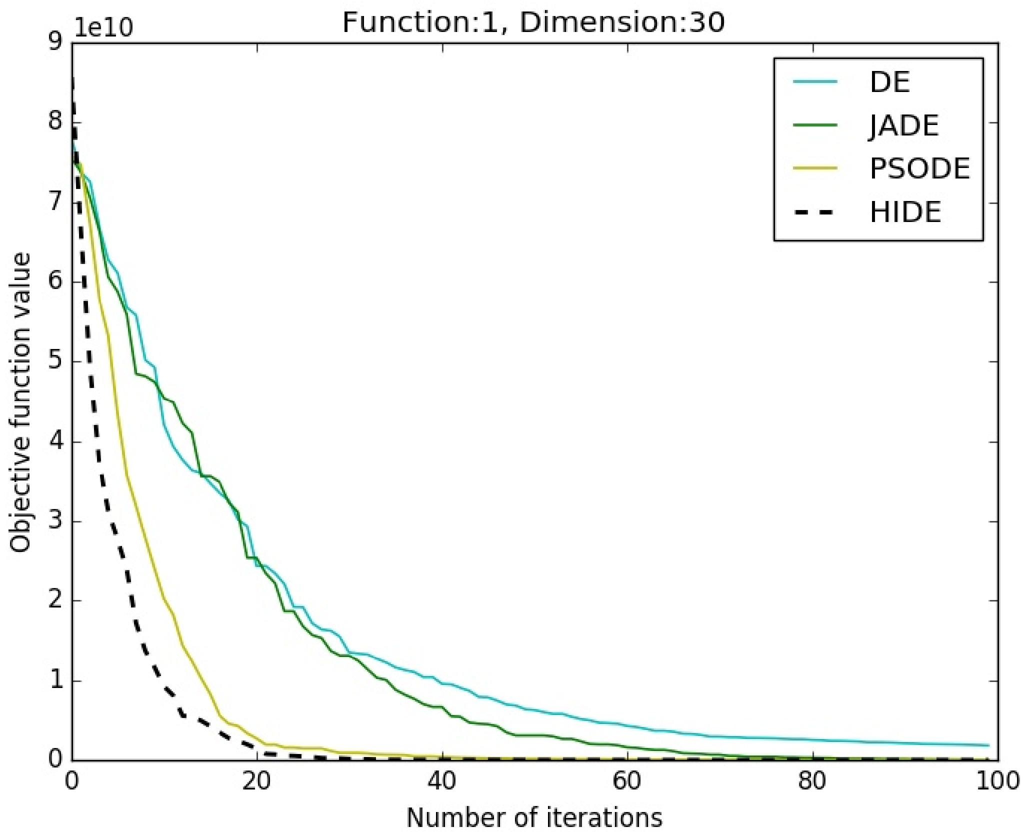

Figure 5

0.24